CONTROL OF THE ACCELERATION REGION IN HALL THRUSTERS

David Staack, Yevgeny Raitses and Nathaniel J. Fisch
Princeton Plasma Physics Laboratory
Princeton, NJ 08543

Abstract

An inward shift of the location of the acceleration regions and an increase in the discharge current are observed when graphite electrodes are placed along the ceramic channel of a Hall thruster. These changes correlate with each other and with currents collected from the plasma by the electrodes. A simplified numerical analysis showed that the conductivity of the electrode can potentially contribute to these changes, but not sufficient to explain measured currents through the electrode.

Introduction

The effect of material properties of the channel walls on Hall thruster operation was studied elsewhere (See, for example, Refs. 1-7 for ceramic materials and Refs.7-9 for conductive materials). A Hall thruster with segmented electrodes along the thruster channel can have certain advantages over conventional non-segmented thruster configurations, particularly with regard to plume divergence, thruster lifetime and thruster compatibility with satellite. Electrodes made from conductive materials can be emissive[1,9] or non-emissive[9,10]. In our previous works with non-emissive electrodes the effect on the plasma potential distribution and plume angle were already measured and to some extent explained by lower secondary electron emission (SEE) from metal electrodes as compared to ceramic channel walls.[11] We have also previously considered the electrode conductivity and a plasma collecting role of the electrode as causing the measured effects of the electrodes on the plasma potential distribution.[10-12] This paper focuses on the measured changes to the discharge current and potential profiles induce by conducting segmented electrodes and how these effects can be related to the measured and estimated currents through the conducting electrode.

Experimental Setup

Experiments investigating the effects of segmented electrodes in Hall thruster were performed with the PPPL 90mm Hall thruster, shown in Fig. 1. The details of the experiment and setup are described elsewhere.[10-14] An emissive probe mounted on a high-speed reciprocating positioning system was used to measure the plasma potential for a conventional hall thruster and a segmented Hall thruster with the electrode in floating and cathode biased conditions. Plasma potential profiles were measured for conventional thruster configuration without segmented electrode (WS) and for several segmented configurations, namely, with a floating inner wall electrode (NS), a cathode biased inner wall electrode (BNS), floating inner wall and floating outer wall electrodes (NSO), and biased inner wall and floating outer wall electrodes (BNSO). Fig. 2 is a sketch of the location of the inner and outer-segmented electrodes relative to the thruster and magnetic field lines. The inner electrode is 4 mm long and the outer electrode is 8 mm long.
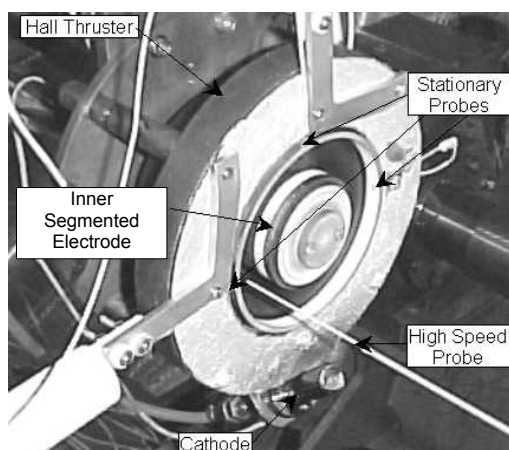

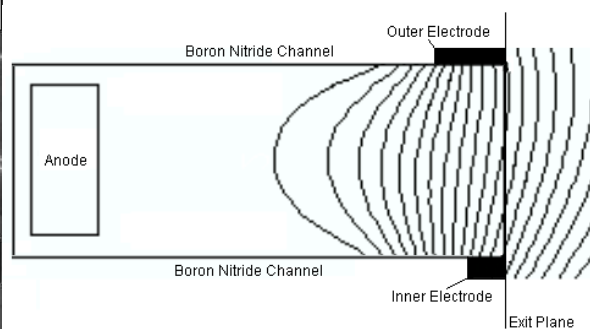Figure 1: PPPL 90 mm Hall thruster experimental setup.

Figure 2: Location of electrodes

Results and Discussions

Fig. 3 shows the measured plasma potential profiles for the five electrode configurations. The thruster exit plane is located at 46 mm relative to the anode and the plasma potential is in volts relative to the cathode. These measurements were taken at the middle of the thruster channel. As can be seen, the use of electrodes on the inner and outer walls and the biasing of the inner electrode cause inward shifts of the plasma potential profiles. For the thruster configurations with one segmented electrode on the inner wall the shift in the acceleration region was smaller at the middle of the channel than at other radial locations. This is due to the appearance of a "jet" like protrusion, described in Refs. 10, 15. Nevertheless, for the purpose of the comparison between different one segmented and two segmented electrode configurations it seems more reasonable to use these results measured along the thruster median. For all thruster configurations the discharge voltage was 250V, the xenon flow rate was 1.7 mg/s and the magnetic field and cathode flow rate were constant. The discharge currents for non-segmented, one–segmented (floating inner, biased inner) and two segmented with an additional floating electrode on the outer wall (inner floating and inner biased) were 1.59, 1.62, 1.65, 1.70, and 1.72, respectively.
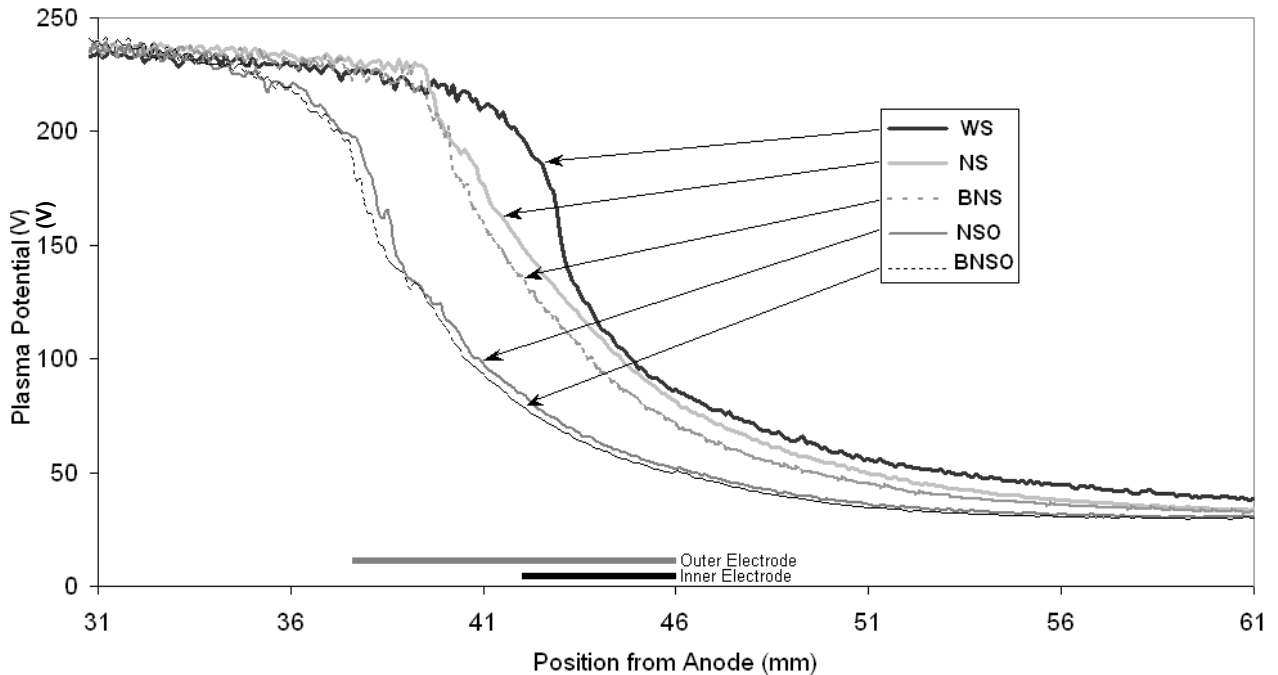

Figure 3: Potential profile distributions measured at the middle of the channel for convention thruster without segmented electrode (WS), with a floating inner wall electrode (NS), a cathode biased inner wall electrode (BNS), floating inner wall and floating outer wall electrodes (NSO), and biased inner wall and floating outer wall electrodes (BNSO).

We shall now analyze these experimental results considering for simplicity only differences in the conductive properties of the electrode and channel wall materials at steady state operation. For dielectric wall materials the ion and electron fluxes to the wall must be equal locally to provide zero net current. For conductive walls the ion and electron fluxes need not be equal integrally since electrons can freely move within the conductor. This difference introduced by the conductivity of the electrode becomes important when the electrode *sees* a significant gradient in plasma along its surface, which must be equipotential. Because of the electron temperature, there is established a sheath, which repels electrons from the plasma. The voltage potential drop in the sheath is lower at the *cathode* end of the electrode than at the *anode end* and therefore, more electrons will be collected at this end. Then, the *anode* end of the electrode will mainly collect ions since it is biased more negative to the plasma, than it would be in the case of a dielectric wall. The excess of electrons collected at the cathode end of the electrode will flow through the electrode to neutralize the ions coming to the anode end of the electrode. On the other hand, the biased electrode collects mainly or only ions when the bias voltage is enough to repel all electrons from the plasma. One can suggest that the segmented electrode acts simply as some sort of a double electrostatic probe at different points of its V-I characteristics: below ion saturation for floating and at saturation for cathode biased.

The currents to and through the electrode can be estimated based upon the measured plasma potential $\Phi_{pl}(z)$ and floating potential $\Phi_{fl}(z)$ profiles and the total ion flux, J_{iT}, measured for the thruster configuration.

For simplicity of these qualitative estimations, the plasma density along the channel was determined as $n_0(z)=J_{iT}/eV_{ion}(z)$, where $V_{ion}(z)=\sqrt{2e\Delta\Phi_{pl}(z)/M_{ion}}$ is the ion velocity and M_{ion} is the atom mass. The other assumptions include: Boltzmann's distribution for the electron density along the magnetic field lines and the Bohm velocity for ions at the sheath edge, $V_{iB}(z)=[kT_e(z)/M_{ion}]^{0.5}$, where $T_e(z)\approx1/2(\Phi_{pl}(z)-\Phi_{fl}(z))/\text{Ln}(M_{ion}/2\pi m_e)$ is the electron temperature derived from cold and hot probe measurements neglecting uncertainties affected by a flowing plasma and double sheath at the hot probe. Then, $J_{er}(z)=1/4en_0(z)\exp[-e(\Phi_{pl}(z)-\Phi_W)/kT_e(z)]V_{eth}(z)$ and $J_{ir}(z)=1/2en_0(z)V_{iB}(z)$, where V_{eth} is the electron thermal velocity. Neglecting the electrical resistance of the electrode and dividing it into finite size elements the net current to each part is $I_f(z) = S(J_{iz}(z) - J_{er}(z))$, where S is the surface area of the electrode element exposed to the plasma. For a floating electrode, we used its potential, Φ_W, as a fitting parameter to fulfill the condition of $\Sigma I_f =0$. The current through the electrode at a given point along its length, $I_r(z)$, can be estimated as a cumulative sum of the net current to each element, $I_r(z)=\sum_{\zeta=a,b}^{z}I_f(\zeta)$, where $z=a$ and $z=b$ are the ends of the electrode. In the case of a biased electrode the current $I_b =\Sigma I_f$ can be estimated for fixed Φ_W. Note that the current collected by the biased electrode and the current through the electrode in the floating case can be close to each other but are not equal because at the cathode side of the floating electrode the collected ions are compensated locally by electron flux from the plasma, and those electrons do not need to flow through the electrode.

For each of the four segmented electrode thruster configurations the current through the electrode was estimated using their respective plasma potential measurements. Fig. 4 shows electrode current, $I_r(z)$, estimations for the floating and biased inner electrodes, the floating inner and floating outer electrodes and for the biased inner and floating outer electrodes. There is a general correlation to the measured trends of Fig. 3. In addition, as seen in Table 1, changes of the discharge current and the location of the acceleration region are larger for the electrode configurations with the larger estimated currents flowing through them. However, some simulated results are underestimated. For the two inner biased configurations the estimated values for the biased current were 2.7 (one segmented) and 4.1 (two segmented) times below than measured results. The estimated floating potentials for the floating configurations were also smaller by 2.7 V (one segmented) and 14.5 V (two segmented).. Obviously, these discrepancies may result from the assumptions of this simplified model in particular, in determination of the plasma density, electron temperature as well as from measured errors of the plasma and floating potentials affected by plasma perturbations.[10, 16]
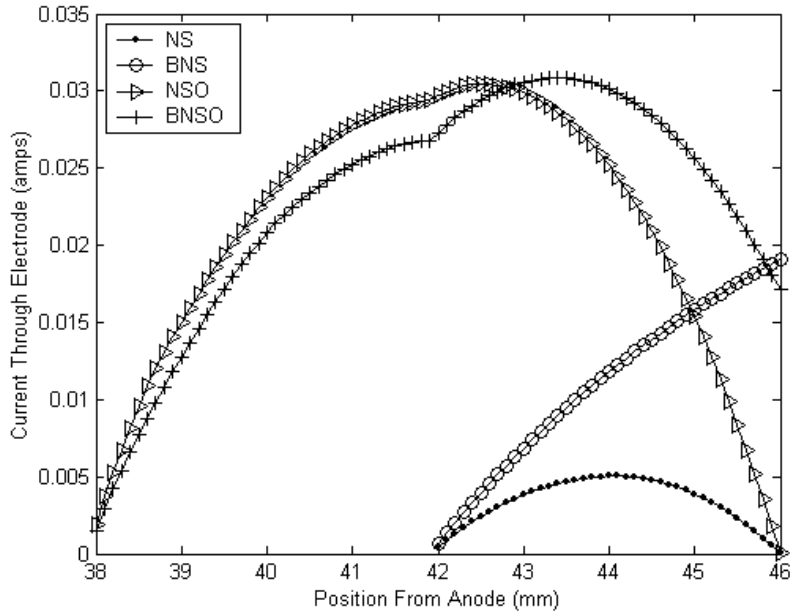

Figure 4: Estimated current through the electrodes for floating inner wall electrode (NS), cathode biased inner wall electrode (BNS), floating inner wall and floating outer wall electrodes (NSO), and biased inner wall and floating outer wall electrodes (BNSO) configurations. The measured currents for the BNS and BNSO cases were 56 mA and 70 mA respectively.

Table 1: Summary of estimated electrode currents and potentials and measured thruster parameter for convention thruster without segmented electrode (WS), with a floating inner wall electrode (NS), a cathode biased inner wall electrode (BNS), floating inner wall and floating outer wall electrodes (NSO), and biased inner wall and floating outer wall electrodes (BNSO). Values marked in bold can be directly compared.

Electrode Configuration	WS	NS	BNS	NSO	BNSO
Measured Discharge Current (A)	1.59	1.62	1.65	1.70	1.72
Increase in Discharge Current from WS (mA)	0	30	60	110	130
Measured Inner Electrode Current (mA)	NA	NA	**56**	NA	**70**
Max. Estimated Inner Electrode Current (mA)	*0*	*5*	***19***	*3*	***17***
Max. Estimated Outer Electrode Current (mA)	*0*	*0*	*0*	*29*	*27*
Max. Estimated Electrode(s) Current (mA)	*0*	*5*	*19*	*30*	*31*
Estimated Electrode Influence Factor (mA*mm)	*0*	*14*	*46*	*170*	*185*
Estimated Outer Electrode Potential (V)	*NA*	*NA*	*NA*	*13.1*	*11.7*
Estimated Inner Electrode Potential (V)	*NA*	***20.8***	*0*	***7.2***	*0*
Measured Inner Electrode Potential (V)	NA	**23.5**	0	**21.7**	0
Location from anode of V_p = 175 V (mm)	42.7	41	40.6	38.1	37.8

Note, the changes in discharge current and plasma potential seen in these experiments are shown to correlate to the amount of current flowing through the electrode. Because of the discharge current continuity, current driven axially through the electrode is current that is no longer going through the plasma. Like a resistor in parallel the electrode shorts a portion of the current in the plasma. Then, it follows from Kirchoff's laws that the shortened current through the electrode would result in 1) an increase of the discharge current, 2) a decrease of the potential drop along the region with the electrode and 3) an increase of the potential drop in the rest regions in which the electrode is not located. Here we assumed that the electron mobility in the thruster plasma is not affected by the presences of the electrodes (e.g. Bohm mobility for the same magnetic field). Based upon this simple electrical analogy and this assumption, the current through the electrode should be greater than the change in discharge current by adding the electrode in parallel. A comparison of the results of Table 1 for the biased inner graphite electrode cases (one segmented and two segmented electrode configurations) shows that the current through the electrode is slightly smaller than an increase of the discharge current relative to the non-segmented configuration. However, in our earlier experiments reported in Ref. 12 with the inner electrode made from molybdenum, which has the same sizes as the graphite inner electrode described here, the increase of the discharge current was clearly smaller than the current measured in the electrical circuit of the biased electrode. It seems, therefore, that there are thruster operating regimes, which are primarily affected by the conductivity of the electrode.

Applying the previous assumption that the electrode does not affect the electron mobility, an increase of the axial electron flux towards the anode can be facilitated by an increase of the electric field in the regions without electrodes, $E = J_e/\mu_\perp$. Since the inner electrode is located between the maximum of the magnetic field and the cathode, the electron mobility is smaller on the anode side of the electrode than between the cathode and the electrode. Therefore, the increase of the electric field inside the channel should be larger than outside. This may explain the inward shift of the acceleration region measured for the segmented electrode configurations as compared to non-segmented thruster.

Interestingly, the same results, including the increase of the discharge current and the inward shift of the acceleration region can also be explained by the effects of SEE[10]. The discharge current increases because of a larger electron temperature, and so higher ionization rate, in the channel with a low SEE electrode as compared to the non-segmented channel made entirely from a ceramic material. In Ref. 17, the thruster with the channel walls made entirely from a conductive material operated with larger electron temperatures than with ceramic channel walls. In general, the experimental results of Ref. 17 for non-segmented thruster configurations appear to be in agreement with simulations of Ref. 2 and relevant also to Ref. 10 for the segmented thruster. The higher ionization rate in the segmented channel leads to larger ion and electron fluxes. Indeed for the two segmented electrode configurations, we measured an increase of the propellant utilization[13,14], but not for the one segmented electrode cases, in which it either dropped or was unchanged[12,14].

Note that an increase of the electron temperature could be also result from lower electron losses on the negatively biased and floating electrodes. However, following the theoretical model of Ref. 3 describing the plasma wall phenomena in conventional Hall thrusters, one can expect that in the one segmented configurations electron losses on the outer ceramic wall opposite to the electrode are still significant because of large SEE that limits the electron temperature. This limit is implied by the charge saturation regime in the

plasma-wall sheath on this wall.[3] In the case of the two-segmented configuration, the same magnetic field lines intersect inner and outer electrodes placed on opposite walls, which are conductive and have low SEE. As a result, electron losses are smaller on both electrode walls as compared to higher SEE ceramic walls and therefore, larger electron temperatures are in principle possible in the two segmented channel. This may explain larger propellant utilization measured for these segmented configurations.

Conclusions

A comparison of measured results for segmented and non-segmented Hall thruster configurations showed that an inward shift of the acceleration region and an increase of the discharge current correlate with the current shorted through the segmented electrode. A simplified model suggests that in addition to a lower secondary electron emission as compared to ceramic channel wall materials, the conductivity of metal electrodes can be responsible for their effects on the thruster operation. Obviously, the precise physics involved in the effects of segmented electrodes is more complicated and may combine SEE, conductivity and other effects. Future work will be aimed at distinguishing between the effects of SEE and conductivity.

Acknowledgements

References

1. A.I. Morozov and V.V. Savelyev, in *Review of Plasma Physics*, edited by B.B. Kadomtsev and V.D. Shafranov, Consultants Bureau, New York, 2000, Vol. 21
2. M. Keidar, I. D. Boyd, and I. I. Beilis, Phys. Plasmas **8**, 5315 (2001).
3. E. Ahedo, Phys. Plasmas **9**, 4340 (2002).
4. J. Fife, M. Martínez-Sánchez, and J. Szabo, in *33rd Joint Propulsion Conference, Seattle, WA* (American Institute of Aeronautics and Astronautics, Washington, D.C., 1997), AIAA 97-3052.
5. L. Jolivet and J.-F. Roussel, in *SP-465: 3rd Spacecraft Propulsion Conference, Cannes* (Francia) (European Space Agency, Noordwijk, The Netherlands, 2000), pp. 367–376.
6. A. Fruchtman and N. J. Fisch, AIAA paper 98-3500, Celevelan, OH 1998.
7. G. E. Bugrov, V. A. Ermolenko and V. K. Charchevnikov, Formation of Electron Distribution Function in Hall Thrusters with Dielectric and Metal Walls, the 6th All-Union Conference on Plasma Accelerators and Ion Injectors, Dnepropetrovsk, 1986, pp 33-34 [in Russian]
8. V. V. Egorov, V. Kim, A. A. Semenov and I. I. Shkarban, in *Ion Injectors and Plasma Accelerators*, Energoizdat, Moscow, 1990, p. 56 [in Russian].
9. S. Barral, K. Makowski, and Z. Peradzynski, N. Gascon, M. Dudeck, "Model of Stationary Plasma Thruster with Conducting Walls", AIAA 2002-4245, 38th Joint Propulsion Conference, Indianapolis IN.
10. Y. Raitses, D. Staack and N. J. Fisch, "Plasma Characterization of Hall Thruster with Active and Passive Segmented Electrodes", AIAA 2002-3954, 38th Joint Propulsion Conference, Indianapolis, IN.
11. Y. Raitses, M. Keidar, D. Staack and N. J. Fisch, "Effect of segmented electrodes on Hall thruster Plasma" J. Appl Phys 92 (9): 4906-4911 Nov, 2002.
12. Y. Raitses, L. A. Dorf, A. A. Litvak and N. J. Fisch, J. Appl. Phys. 88, 1263, 2000.
13. N. Fisch, Y. Raitses, L. A. Dorf and A. A. Litvak, J. Appl. Phys. 89, 2040, 2001.
14. Y. Raitses, D. Staack and N. J. Fisch, "Measurements of Plasma Potential Distribution in Segmented Electrode Hall Thruster", IEPC-01-060, the 27th Inter. Electric Propulsion Conf, Pasadena, CA 2001.
15. J. M. Haas and A. D. Gallimore, Phys. Plasmas, **8**, 652, 2001
16. D. Staack, Y. Raitses, and N. J. Fisch, "Investigations of Probe Induced Perturbations in a Hall Thruster", AIAA 2002-4109, 38th Joint Propulsion Conference, Indianapolis, IN.
17. S. A. Chartov, Effect of the channel material on integral characteristics of Hall thrusters, the 6th All-Union Conference on Plasma Accelerators and Ion Injectors, Dnepropetrovsk, 1986, pp 33-34 [in Russian]